Characterizing the Uncertainty of the Fundamental Matrix

Article *in* Computer Vision and Image Understanding · September 1995

DOI: 10.1006/cviu.1997.0531 · Source: CiteSeer

6 authors, including:

Gabriela Csurka
Xerox Corporation
126 PUBLICATIONS **4,430** CITATIONS
SEE PROFILE

Zhengyou Zhang
Microsoft
336 PUBLICATIONS **20,532** CITATIONS
SEE PROFILE

Olivier D. Faugeras
National Institute for Research in Computer Sci…
543 PUBLICATIONS **29,579** CITATIONS
SEE PROFILE

INRIA

INSTITUT NATIONAL DE RECHERCHE EN INFORMATIQUE ET EN AUTOMATIQUE

Characterizing the Uncertainty of the Fundamental Matrix

Gabriella CSURKA

Cyril ZELLER

Zhengyou ZHANG

Olivier FAUGERAS

N° 2560

Juin 1995

PROGRAMME 4

ISSN 0249-6399

INRIA
SOPHIA ANTIPOLIS

Characterizing the Uncertainty of the Fundamental Matrix

Gabriella CSURKA
Cyril ZELLER
Zhengyou ZHANG
Olivier FAUGERAS

Programme 4 — Robotique, image et vision
Projet Robotvis

Rapport de recherche n ° 2560 — Juin 1995 — 29 pages

Abstract: This paper deals with the analysis of the uncertainty of the fundamental matrix. The basic idea is to compute the fundamental matrix and its uncertainty in the same time. We shall show two different methods.

The first one is a statistical approach. As in all statistical methods the precision of the results depends on the number of analyzed samples. This means that we can always improve our results if we increase the number of samples but this process is very time consuming.

We propose a much simpler method which gives results which are close to the results of the statistical methods.

At the end of paper we shall show some experimental results obtained with synthetic and real data.

Key-words: Epipolar geometry, Fundamental matrix, Uncertainty, Covariance matrix

(Résumé : tsvp)

Unité de recherche INRIA Sophia-Antipolis
2004 route des Lucioles, BP 93, 06902 SOPHIA-ANTIPOLIS Cedex (France)
Téléphone : (33) 93 65 77 77 – Télécopie : (33) 93 65 77 65

Caractérisation de l'incertitude de la matrice fondamentale

Résumé : Ce papier propose une analyse de l'incertitude liée à la matrice fondamentale. L'idée de base est de calculer la matrice fondamentale et son incertitude en même temps. Nous montrons deux méthodes différentes.

La première est une méthode statistique. Elle ne donne donc de résultats précis qu'au prix de l'analyse d'un grand nombre de réalisations, ce qui en fait une méthode coûteuse en temps.

La seconde est une méthode analytique. Elle est trés peu coûteuse en temps mais approximative. Nous montrons dans ce papier, à partir d'images synthétiques comme d'images réelles, qu'elle donne cependant des résultats suffisamment proches de ceux de la méthode statistique pour être utilisée dans la pratique.

Mots-clé : Géométrie épipolaire, Matrice fondamentale, Incertitude, Matrice de covariance

Contents

1 Introduction

The study of the fundamental matrix is very recent in computer vision. It was introduced in **[FLM92]** as a generalisation of the essential matrix described in **[LH81]** to uncalibrated images. The importance of the fundamental matrix becomes evident in the case of two the uncalibrated cameras. In this case the fundamental matrix is the key concept, as it contains all the geometrical information relating two different images. It determines and is determined by the positions of the two epipoles and the epipolar transformation mapping an epipolar line of the first image to its corresponding epipolar line in the second image. It can be computed from a certain number of point correspondences obtained from the pair of images using some correlation based algorithms, independently of any other knowledge about the world.

In the first part of this paper we describe some methods to compute the fundamental matrix from a pair of images assuming that some image point correspondences are known. The methods are not detailed more than necessary because they have been already presented in the literature (**[Luo92, HGC92, Ols92, Har95]**).

In the second part two different methods are presented to compute the covariance matrix of the fundamental matrix. The stability of the fundamental matrix has already been studied by Q.-T.Luong (**[Luo92]**, **[LF94]**), but the corresponding covariance matrix was not accurately estimated, in particular the variances were too much overestimated to be used in further computations.

We shall show in the last part of this report that using the two methods we propose we obtain a much better estimation of the uncertainty of the fundamental matrix.

2 The fundamental matrix

The camera model used is the classical *pinhole model*. If the object space is considered to be the 3-dimensional Euclidean space $\mathcal{R}^3$ embedded in the usual way in the 3-dimensional projective space $\mathcal{P}^3$ and the image space the 2-dimensional Euclidean space $\mathcal{R}^2$ embedded in the usual way in the 2-dimensional projective space $\mathcal{P}^2$, the camera is then described as a *linear projective application* from $\mathcal{P}^3$ to $\mathcal{P}^2$ (see [Fau93]). If we denote by $\check{\mathbf{P}}$ the 3×4-matrix representing this application, we have:

$$\lambda \mathbf{m} = \underbrace{\left[\begin{array}{cc} \mathbf{P} & \mathbf{p} \end{array} \right]}_{\check{\mathbf{P}}} \mathbf{M} \tag{1}$$

where $\mathbf{p}$ denotes the last column of $\check{\mathbf{P}}$, $\mathbf{M} = [X, Y, Z, 1]^T$ represents an object point M, $\mathbf{m} = [x, y, 1]^T$, its projection m onto the image and λ a nonzero scalar. We assume $rank(\mathbf{P}) = 3$.

If we have two cameras, represented by $\check{\mathbf{P}}$ and $\check{\mathbf{P}}'$, by eliminating $\mathbf{M}$ from equation (1), we obtain the relation between the projections of M onto the first and second image:

$$\lambda' \mathbf{m}' = \lambda \mathbf{H} \mathbf{m} + \mathbf{e}' \tag{2}$$

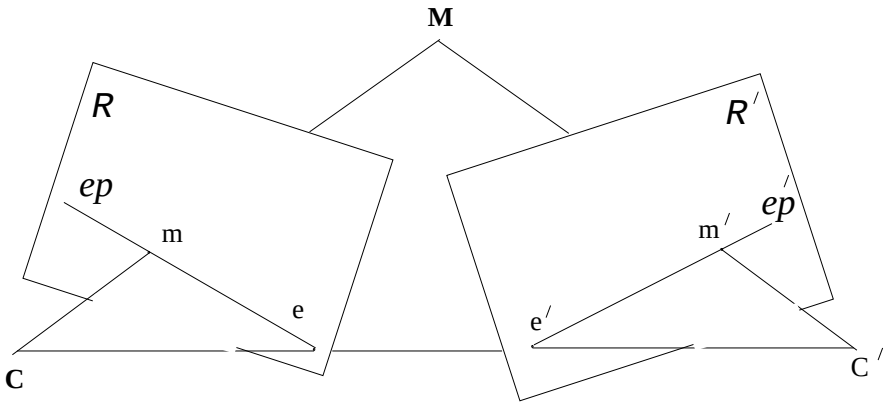

Figure 1: The epipolar geometry.

where $\mathbf{H} = \mathbf{P}'\mathbf{P}^{-1}$ and $\mathbf{e}' = \mathbf{p}' - \mathbf{H}\mathbf{p}$. Equation (2) means that m' lies on the line called the *epipolar line* of m, going through the point represented by $\mathbf{e}'$, the *epipole*, and the point represented by $\mathbf{Hm}$. This line is represented by the vector $\mathbf{Fm}$ such that:

$$\mathbf{F} = [\mathbf{e}']_\times \mathbf{H} \tag{3}$$

where $[\mathbf{e}']_\times$ is a 3×3 matrix representing the cross-product with the vector $\mathbf{e}'$ ($[\mathbf{e}']_\times \mathbf{x} = \mathbf{e}' \times \mathbf{x}$).

$\mathbf{F}$ is the *fundamental matrix* which describes this correspondence between an image point in the first image and its epipolar line in the second (see also **[Luo92]**). It is of rank 2 because $[\mathbf{e}']_\times$ is an antisymmetric matrix which leads to $det(\mathbf{F}) = 0$. Its eigenvector associated to the zero eigenvalue is the epipole of the first image represented by:

$$\mathbf{e} = \mathbf{H}^{-1}\mathbf{p}' - \mathbf{p}$$

Geometrically (see figure 1), we see that, as M lies, by definition, on the line (Cm), its projection m' necessarily lies on the image of (Cm) by the second camera, that is the epipolar line. Moreover, all the epipolar lines go through a same point, the epipole, which is the image of C by the second camera.

Then pairs (m, m') of corresponding points satisfy:

$$\mathbf{m}'^T \mathbf{F}\mathbf{m} = 0 \tag{4}$$

3 Computing the fundamental matrix

Assuming that some image point correspondences, represented by $(\mathbf{m}'_i, \mathbf{m}_i)$, have been found, as described in (**[Luo92, ZDFL94]**), for example, the fundamental matrix $\mathbf{F}$ is computed,

up to a nonzero scalar factor, as the unique solution of the system of equations, derived from equation (3):

$$\mathbf{m}_i'^T \mathbf{F} \mathbf{m}_i = 0 \tag{5}$$

This system can be solved as soon as seven such correspondences are available: only eight coefficients of $\mathbf{F}$ need to be computed, since $\mathbf{F}$ is defined up to a nonzero scalar factor, while equation (5) supplies one scalar equation per correspondence and $\det(\mathbf{F}) = 0$, the eighth. If there are more correspondences available, which are not exact, as it is the case in practice, the goal of the computation is to find the matrix which approximates best the solution of this system according to a given criterion. A more detailed study is to be found in ([**Luo92**]).

3.1 The linear criterion

Denoting by F_{ij} the coefficient of $\mathbf{F}$ located at line i and column j, x_i, y_i and x_i', y_i' the image coordinates of $\mathbf{m}_i$ and $\mathbf{m}_i'$ respectively, equation (5) is rewritten:

$$\begin{aligned} \mathbf{u}^T \mathbf{f} &= 0 \qquad \text{with} \\ \mathbf{u} &= [x_i x_i', y_i x_i', x_i', x_i y_i', y_i y_i', y_i', x_i, y_i, 1] \\ \mathbf{f} &= [F_{11}, F_{12}, F_{13}, F_{21}, F_{22}, F_{23}, F_{31}, F_{32}, F_{33}] \end{aligned} \tag{6}$$

The scalar equation (6) is linear homogeneous in $\mathbf{f}$. Thus, eight correspondences allow to determine $\mathbf{F}$, up to a nonzero scalar factor. This approach, known as the *eight points algorithm*, was introduced by Longuet-Higgins ([**LH81**]).

If more than eight correspondences are available, say n, the use of equation (6) as a criterion leads to a linear least squares problem, that is the minimization of:

$$\sum_{i=1}^{n} ((\mathbf{m}_i')^T \mathbf{F} \mathbf{m}_i)^2 \tag{7}$$

which is solved the usual way: the solution is the eigenvector of:

$$\mathbf{U}\mathbf{U}^T \qquad \text{where} \qquad \mathbf{U} = \left[\ \mathbf{u}_i \ \right]_{i=1,\ldots,n}$$

associated with the smallest eigenvalue.

The advantage of the linear criterion is that it leads to a non-iterative computation method and its disadvantage, is that it is quite sensitive to noise, even with a large set of data points. This is due to the fact, on the one hand, that the constraint $\det(\mathbf{F}) = 0$ is not necessarily satisfied and, on the other hand, that the criterion is not normalized.

3.2 The nonlinear criterion

3.2.1 A parameterization of the fundamental matrix

Definition. As underlined above, the use of the linear criterion does not take into account the rank constraint on the fundamental matrix. One way to do this is to parameterize the

problem such that we are only searching for the right matrix among the 3×3-matrices of rank 2.

Denoting the columns of $\mathbf{F}$ by the vectors $\mathbf{c}_1$, $\mathbf{c}_2$ and $\mathbf{c}_3$, we have :

$$\begin{array}{rcl} Rank(\mathbf{F}) & = & 2 \\ & \Longleftrightarrow & \\ (\exists j_0 \in [1,3]) \ (\exists \lambda_1, \lambda_2 \in \mathcal{R}), & & \mathbf{c}_{j_0} + \lambda_1 \mathbf{c}_{j_1} + \lambda_2 \mathbf{c}_{j_2} = 0 \quad (8) \\ (\nexists \lambda \in \mathcal{R}), & & \mathbf{c}_{j_1} + \lambda \mathbf{c}_{j_2} = 0 \quad (9) \end{array}$$

Condition (9), as a non-existency condition, cannot be expressed by a parametrization: we shall only keep condition (8) and so extend the parametrized set to all the 3×3-matrices of rank strictly less than 3. A parametrization of $\mathbf{F}$ is then given by $(\mathbf{c}_{j_1}, \mathbf{c}_{j_2}, \lambda_1, \lambda_2)$. This parametrization implies to divide the parametrized set among three maps, corresponding to $j_0 = 1$, $j_0 = 2$ and $j_0 = 3$. Indeed, the matrices of rank 2 having, for example, the following forms :

$$\left[\begin{array}{ccc} \mathbf{c}_1 & \mathbf{c}_2 & \lambda \mathbf{c}_2 \end{array} \right] \text{ and } \left[\begin{array}{ccc} \mathbf{c}_1 & \mathbf{0}_3 & \mathbf{c}_3 \end{array} \right] \text{ and } \left[\begin{array}{ccc} \mathbf{c}_1 & \mathbf{c}_2 & \mathbf{0}_3 \end{array} \right]$$

have no parametrization if we take $j_0 = 1$.

Obviously, the 3-vector whose coordinates are λ_1, λ_2, in this order, and 1 at the j_0^{th}, position is the eigenvector of $\mathbf{F}$, thus the epipole in the case of the fundamental matrix. Using such a parametrization implies to directly compute the epipole which is often the useful quantity, instead of the matrix itself.

To make the problem symmetrical and since the epipole in the other image is also worth being computed, the same decomposition as for the columns is used for the rows, which divides the parametrized set into 9 maps, corresponding to the choice of a column and a row as linear combinations of the two columns and two rows left. A parametrization of the matrix is then formed by the two coordinates x and y of the first epipole, the two coordinates x' and y' of the second epipole and the four elements a, b, c and d left by $\mathbf{c}_{i_1}$, $\mathbf{c}_{i_2}$, $\mathbf{l}_{j_1}$ and $\mathbf{l}_{j_2}$, which in turn parametrize the epipolar transformation mapping an epipolar line of the first image to its corresponding epipolar line in the second image. In that way, the matrix is written, for example, for $i_0 = 3$ and $j_0 = 3$:

$$\mathbf{F} = \left[\begin{array}{ccc} a & b & -ax - by \\ c & d & -cx - dy \\ ax' + cy' & bx' + dy' & -(ax + by)x' - (cx + dy)y' \end{array} \right] \quad (10)$$

At last, to take into account the fact that the fundamental matrix is defined only up to a scale factor, the matrix is normalized by dividing the four elements defining the epipolar transformation by the biggest in absolute value.

Choosing the best map. Giving a matrix $\mathbf{F}$ and the epipoles, or an approximation of it, we must be able to choose, among the different maps of the parametrization, the most suitable for $\mathbf{F}$. Denoting by $\mathbf{f}_{i_0 j_0}$ the vector of the elements of $\mathbf{F}$ once decomposed like in

equation (10), i_0 and j_0 are chosen in order to maximize the rank of the 9×8 jacobian matrix:

$$\mathbf{J} = \frac{d\mathbf{f}_{i_0 j_0}}{d\mathbf{p}} \quad \text{where} \quad \mathbf{p} = [x, y, x', y', a, b, c, d]^T \tag{11}$$

This is done by maximizing the norm of the vector whose coordinates are the determinants of the nine 8×8-submatrices of $\mathbf{J}$. An easy calculation shows that this norm is equal to:

$$(ad - bc)^2 \sqrt{x^2 + y^2 + 1}\sqrt{x'^2 + y'^2 + 1}$$

3.2.2 The criterion

Using the parametrization above makes the equation (5) no longer linear in $\mathbf{F}$ and thus leads to a nonlinear least squares problem: the minimization of (7) must proceed iteratively.

As the linearity is lost anyway, we can tackle the problem of the normalization of the criterion underlined above. This is done by minimizing the sum of the squares of the distance of m to the epipolar line of m' and the distance of m' to the epipolar line of m:

$$\sum_{i=1}^{n} C_i^2 \tag{12}$$

where

$$C_i^2 = \left(\frac{1}{[\mathbf{F}\mathbf{m}_i]_x^2 + [\mathbf{F}\mathbf{m}_i]_y^2} + \frac{1}{[\mathbf{F}^T\mathbf{m}'_i]_x^2 + [\mathbf{F}^T\mathbf{m}'_i]_y^2} \right) (\mathbf{m}_i'^T \mathbf{F}\mathbf{m}_i)^2$$

so that multiplying $\mathbf{F}$ by a nonzero scalar does not change the value of the sum.

The minimization is performed by a classical Levenberg-Marquardt method (see [PFTV88]). During the process of minimization, the parametrization of $\mathbf{F}$ is susceptible of change: the parametrization chosen for the matrix at the beginning of the process is not necessarily the most suitable for the final matrix.

3.3 The outliers rejection method

An outliers rejection method is used to eliminate some possible outliers among the correspondences. The technique exploited is the least median squares, which is described in detail in [ZDFL94].

4 The covariance matrix

In order to quantify the uncertainty related to the estimation of the fundamental matrix by the method described in section **3.2.2**, we modelize the fundamental matrix as a random vector $\mathbf{f}$ of R^7 whose mean is the exact value we are looking for. Each estimation is then assimilated to a realization of $\mathbf{f}$ and the uncertainty is given by the covariance matrix of $\mathbf{f}$.

We recall, in this section, the usual techniques used to estimate the covariance matrix of a random vector $\mathbf{y}$ of R^p and to graphically represent the uncertainty from the covariance matrix.

4.1 Computing the covariance matrix

The covariance of $\mathbf{y}$ is defined by the positive symmetric matrix

$$\Lambda_{\mathbf{y}} = E[(\mathbf{y} - E[\mathbf{y}])(\mathbf{y} - E[\mathbf{y}])^T] \tag{13}$$

where $E[\mathbf{y}]$ denotes the mean of the random vector $\mathbf{y}$.

4.1.1 The statistical method

The statistical method consists in using the well-known law of the large numbers to approximate the mean: if we have a large enough number N of realizations $\mathbf{y}_i$ of a random vector $\mathbf{y}$, then $E[\mathbf{y}]$ can be approximated by the discrete mean

$$E_N[\mathbf{y}_i] = \frac{1}{N}\sum_{i=1}^{N} \mathbf{y}_i$$

and Λ_y is then approximated by

$$E_N[(\mathbf{y}_i - E_N[\mathbf{y}_i])(\mathbf{y}_i - E_N[\mathbf{y}_i])^T] \tag{14}$$

4.1.2 The analytical method

The general case. We now take into account the fact that $\mathbf{y}$ is computed from another random vector $\mathbf{x}$ of R^m using a C^1 function φ:

$$\mathbf{y} = \varphi(\mathbf{x})$$

Writing the first order Taylor expansion of φ in the neighborhood of $E[\mathbf{x}]$ yields to:

$$\varphi(\mathbf{x}) = \varphi(E[\mathbf{x}]) + D\varphi(E[\mathbf{x}]) \cdot (\mathbf{x} - E[\mathbf{x}]) + \varepsilon(\|\mathbf{x} - E[\mathbf{x}]\|^2) \tag{15}$$

where the function $t \to \varepsilon(t)$ from R into R^p is such that $\lim_{t\to 0} \varepsilon(t) = 0$. By considering now that any realization of $\mathbf{x}$ is sufficiently close to $E[\mathbf{x}]$, we can approximate φ by the first order terms of equation (15) which yields:

$$\begin{aligned} E[\mathbf{y}] &\simeq \varphi(E[\mathbf{x}]) \\ \varphi(\mathbf{x}) - \varphi(E[\mathbf{x}]) &\simeq D\varphi(E[\mathbf{x}]) \cdot (\mathbf{x} - E[\mathbf{x}]) \end{aligned}$$

We have then

$$\begin{aligned} E[(\varphi(\mathbf{x}) - \varphi(E[\mathbf{x}]))(\varphi(\mathbf{x}) - \varphi(E[\mathbf{x}]))^T] &\simeq E[D\varphi(E[\mathbf{x}])(\mathbf{x} - E[\mathbf{x}])(\mathbf{x} - E[\mathbf{x}])^T D\varphi(E[\mathbf{x}])^T] \\ &= D\varphi(E[\mathbf{x}])E[(\mathbf{x} - E[\mathbf{x}])(\mathbf{x} - E[\mathbf{x}])^T]D\varphi(E[\mathbf{x}])^T \end{aligned}$$

which gives us a first order approximation of the covariance matrix of $\mathbf{y}$ in function of the covariance matrix of $\mathbf{x}$:

$$\Lambda_{\mathbf{y}} = D\varphi(E[\mathbf{x}])\Lambda_{\mathbf{X}}D\varphi(E[\mathbf{x}])^T \tag{16}$$

The case of an implicit function. In some cases, φ is implicit and we have to make use of the well-known implicit functions theorem to obtain the following result (see chapter 6 of [**Fau93**]).

Proposition 1 *Let a criterion function $C : R^m \times R^p \rightarrow R$ be a function of class C^∞, $\mathbf{x}_0 \in R^m$ be the measurement vector and $\mathbf{y}_0 \in R^p$ be a local minimum of $C(\mathbf{x}_0, \mathbf{z})$. If the Hessian $\mathbf{H}$ of C with respect to $\mathbf{z}$ is invertible at $(\mathbf{x}, \mathbf{z}) = (\mathbf{x_0}, \mathbf{y}_0)$ then there exists an open set U' of R^m containing $\mathbf{x}_0$ and an open set U'' of R^p containing $\mathbf{y}_0$ and a C^∞ mapping $\varphi : R^m \rightarrow R^p$ such that for $(\mathbf{x}, \mathbf{y})$ in $U' \times U''$ the two relations "$\mathbf{y}$ is a local minimum of $C(\mathbf{x}, \mathbf{z})$ with respect to $\mathbf{z}$" and $\mathbf{y} = \varphi(\mathbf{x})$ are equivalent. Furthermore, we have the following equation:*

$$D\varphi(\mathbf{x}) = -\mathbf{H}^{-1}\frac{\partial \mathbf{\Phi}}{\partial \mathbf{x}} \tag{17}$$

where

$$\mathbf{\Phi} = (\tfrac{\partial C}{\partial \mathbf{z}})^T$$
$$\mathbf{H} = \tfrac{\partial \mathbf{\Phi}}{\partial \mathbf{z}}$$

Taking $\mathbf{x}_0 = E[\mathbf{x}]$ and $\mathbf{y}_0 = E[\mathbf{y}]$, equation (16) then becomes

$$\Lambda_{\mathbf{y}} = \mathbf{H}^{-1}\frac{\partial \mathbf{\Phi}}{\partial \mathbf{x}}\Lambda_{\mathbf{X}}\frac{\partial \mathbf{\Phi}}{\partial \mathbf{x}}^T\mathbf{H}^{-T} \tag{18}$$

The case of a sum of squares of implicit functions. If C is of the form:

$$\sum_{i=1}^{n} C_i^2$$

we have:

$$\begin{aligned}
\mathbf{\Phi} &= 2\sum_i C_i\frac{\partial C_i}{\partial \mathbf{z}}^T \\
\mathbf{H} = \frac{\partial \mathbf{\Phi}}{\partial \mathbf{z}} &= 2\sum_i \frac{\partial C_i}{\partial \mathbf{z}}^T\frac{\partial C_i}{\partial \mathbf{z}} \quad \text{to the first order} \\
\frac{\partial \mathbf{\Phi}}{\partial \mathbf{x}} &= 2\sum_i \frac{\partial C_i}{\partial \mathbf{z}}^T\frac{\partial C_i}{\partial \mathbf{x}} \quad \text{to the first order}
\end{aligned}$$

Equation (18) then becomes:

$$\begin{aligned}\Lambda_{\mathbf{y}} &= 4\mathbf{H}^{-1}\sum_i \frac{\partial C_i}{\partial \mathbf{z}}^T \frac{\partial C_i}{\partial \mathbf{x}} \Lambda_{\mathbf{X}} \frac{\partial C_i}{\partial \mathbf{x}}^T \frac{\partial C_i}{\partial \mathbf{z}} \mathbf{H}^{-T} \\ \Lambda_{\mathbf{y}} &= 4\mathbf{H}^{-1}\sum_i \frac{\partial C_i}{\partial \mathbf{z}}^T \Lambda_{C_i} \frac{\partial C_i}{\partial \mathbf{z}} \mathbf{H}^{-T}\end{aligned}$$

Considering that the mean of the value of C_i at the minimum is zero and under the somewhat strong assumption that the C_i's are independent and have identical distributed errors[1], we can then approximate Λ_{C_i} by its sample variance:

$$\frac{S}{n-p}$$

where S is the value of the criterion C at the minimum. Although it has little influence when n is big, the inclusion of p in the formula above aims to correct the effect of a small sample set. Indeed, for $n = p$, we usually always can find an estimate of $\mathbf{y}$ such that $C_i = 0$ for all i, which makes the estimation of the variance using this formula, senseless.

Equation (18) then finally becomes

$$\Lambda_{\mathbf{y}} = \frac{2S}{n-p}\mathbf{H}^{-1}\mathbf{H}\mathbf{H}^{-T} = \frac{2S}{n-p}\mathbf{H}^{-T} \tag{19}$$

4.2 The hyper-ellipsoid of uncertainty

If we define the random vector χ by:

$$\chi = \Lambda_{\mathbf{y}}^{-\frac{1}{2}}(\mathbf{y} - E[\mathbf{y}])$$

and consider that $\mathbf{y}$ follows a Gaussian distribution, then χ follows a Gaussian distribution of mean zero and of covariance:

$$E[\chi\chi^T] = E[\Lambda_{\mathbf{y}}^{-\frac{1}{2}}(\mathbf{y} - E[\mathbf{y}])(\mathbf{y} - E[\mathbf{y}])^T\Lambda_{\mathbf{y}}^{-\frac{1}{2}}] = \Lambda_{\mathbf{y}}^{-\frac{1}{2}}\Lambda_{\mathbf{y}}\Lambda_{\mathbf{y}}^{-\frac{1}{2}} = I$$

Consequently, the random variable $\delta_{\mathbf{y}}$ defined by:

$$\delta_{\mathbf{y}} = \chi^T\chi = (\mathbf{y} - E[\mathbf{y}])^T\Lambda_{\mathbf{y}}^{-1}(\mathbf{y} - E[\mathbf{y}])$$

follows a χ^2 distribution of r degrees of freedom, where r is the rank of $\Lambda_{\mathbf{y}}$ (see [ZF92]). Given a scalar k, we thus know the probability, equal to $P_{\chi^2}(k, r)$, that $\delta_{\mathbf{y}}$ appears between 0 and k^2. In other words, we have the following property:

[1] It is under this assumption that the solution given by the least-squares technique is optimal.

Property 1 *If we consider that* $\mathbf{y}$ *follows a Gaussian distribution, the probability that* $\mathbf{y}$ *lies inside the* k*-hyper-ellipsoid defined by the equation*

$$(\mathbf{y} - E[\mathbf{y}])^T \Lambda_{\mathbf{y}}^{-1} (\mathbf{y} - E[\mathbf{y}]) = k^2$$

where k *is any scalar, is equal to*

$$P_{\chi^2}(k, r)$$

where r *is the rank of* $\Lambda_{\mathbf{y}}$.

The k-hyper-ellipsoid makes possible to graphically represent the uncertainty related to $\Lambda_{\mathbf{y}}$. For that, we usually come down to the bi- or tridimensional case by choosing two or three coordinates of $\mathbf{y}$ and extracting from $\Lambda_{\mathbf{y}}$ the corresponding submatrix, in order to draw an ellipse or an ellipsoid.

5 Experimentation

To compute the covariance matrix of the fundamental matrix, the two methods of section **4** have been tested and compared on both synthetic and real data.

In the case of statistical method, to obtain the N realizations, we added N times independent Gaussian noise of a certain level to the set of image points and computed each time the parameter vectors **f**and the corresponding covariance matrix using the equation (14). Applying this to exact data means that we estimate the exact covariance matrix as best as possible under the condition that we take N large enough. Applying this to real data makes us add noise to data that are already noisy. But, as we shall see when using synthetic data, if the level of noise is not too high, the resulting covariance matrix is still close to the one which is computed from the exact data. This shows us that this method is applicable in the case of real data. The only observation is that it is very costly.

To apply the analytical method, we first observe in the section **3.2.2** that $\mathbf{F}$ is computed using a sum of squares of implicit functions of n point correspondences. Thus, referring to the section **4.1.2**, we have $p = 7$, $m = 4n$ and the criterion function $C(\hat{\mathbf{m}}, \mathbf{f})$, where $\hat{\mathbf{m}} = (\mathbf{m}_1, \mathbf{m}'_1, \cdots, \mathbf{m}_n, \mathbf{m}'_n)^T$ and $\mathbf{f}$ is the vector of the seven chosen parameters for $\mathbf{F}$, is given by equation (12). The analytical method is much faster than the statistical one, but, as it is a first order approximation, it sometimes gives an under-estimation or an over-estimation of the covariance matrix. Nevertheless, the experimental results in the case of synthetic data are good enough to be accepted.

To show the quality of a covariance matrix, we look into what extent the property (1) is verified. For that, we compute 1500 realizations of $\mathbf{f}$ and calculate the ratio of the number of realizations lying inside the k-hyper-ellipsoid to the number of realizations lying outside the k-hyper-ellipsoid. This ratio is then compared to $P_{\chi^2}(k, r)$. Here, $P_{\chi^2}(k, r)$ is taken equal to 0.75, which gives $k = 0.002079$ for $r = 7$, $k = 0.31272$ for $r = 2$ and $k = 0.13862$ for $r = 3$. We have to mention here that the realizations used to compute the above ratios are completely different from the realizations used to compute the covariance matrix of the exact data.

When confronted with real data, we do not have the mean of $\mathbf{f}$ and thus must use the best approximation we have as the center of the hyper-ellipsoid. That is why we also show the quality of the covariance matrix when the center is approximated by the discrete mean of a certain number of realizations of $\mathbf{f}$.

We graphically represent the covariance matrix by showing the ellipses of uncertainty corresponding to the parameters x, y and x', y' (see section 3.2.1), characterizing the epipoles, and the ellipsoid of uncertainty corresponding to the parameters a, b, c, d divided by the biggest in absolute value (see section 3.2.1), characterizing the epipolar transformation.

All this is done for four levels of noise to see how the quality degrades with noise. In order to do this, the points used to compute the fundamental matrix are considered as random vectors following a Gaussian distribution of covariance matrix equal to

$$\sigma^2 \begin{bmatrix} 1 & 0 \\ 0 & 1 \end{bmatrix}$$

The levels of noise correspond to different values of σ. A realization of $\mathbf{f}$ is obtained by computing the fundamental matrix from the realizations of the $2n$ random vectors associated to the points.

5.1 Notations

- $\mathbf{v}$ represent a vector of some parameters of the fundamental matrix. These can be:
  - $\mathbf{e}, \mathbf{e}'$ the parameters corresponding to the epipoles,
  - $\mathbf{h}$ the parameters corresponding to the epipolar transformation
  - $\mathbf{f}$ the vector of the seven parameters.
- M a set of pairs of points (m, m'). We use this notation in the case of the exact data.
- $\mathbf{v}(M)$, the corresponding parameters of the fundamental matrix computed from the set of points M.
- $(M_\sigma)_i$, the i^{th} set of pairs (m_σ, m'_σ). We obtain them by adding independent Gaussian noises of level σ to the points of (m, m') of M for $i = 1, \ldots, n$.
- $\mathbf{v}((M_\sigma)_i)$, the corresponding parameters of the fundamental matrix computed from the sets of points $(M_\sigma)_i$, $i = 1, \ldots, n$.
- $\Lambda(M)$, the covariance matrix computed from the set of points M, using the statistical method. We take the set of exact pairs of points M and, adding noise, we compute the covariance using equation (14) with $\mathbf{y}_i = \mathbf{v}((M_\sigma)_i)$.
- $\Lambda((M_\sigma)_i)$, the covariance matrix computed from the set of points $(M_\sigma)_i$, using the statistical or analytical method. In the case of the statistical method we added again independent noise of level σ to the set of points $(M_\sigma)_i$ and computed the covariance matrix of the parameters $\mathbf{v}((M_\sigma)_i)$.

- $E_n[\mathbf{v}((M_\sigma)_i)]$ the mean of the estimated parameters $\mathbf{v}((M_\sigma)_i)$ from n samples.
- $E_n[\Lambda((M_\sigma)_i)]$ the mean of the corresponding n covariance matrices.

We trace the k-hyper-ellipsoid corresponding to the equation:

$$(\mathbf{y}-\mathbf{v})^T\Lambda_{\mathbf{v}}^{-1}(\mathbf{y}-\mathbf{v}) = k^2$$

where k verifies $P_{\chi^2}(k,r) = p$ for a given p, r beeing the dimension of the vector of parameters $\mathbf{v}$. Taking N different realizations we compute the number of realizations lying inside the k-hyper-ellipsoid. We study the following cases:

- S_0: The k-hyper-ellipsoid corresponding to the covariance matrices $\Lambda(M)$ obtained by the statistical method from the exact data.
- S_i^1: The k-hyper-ellipsoid corresponding to the covariance matrices $\Lambda((M_\sigma)_i)$ obtained by the statistical method centered at the correct value.
- S_n^1: The k-hyper-ellipsoid corresponding to the mean of n covariance matrices $\Lambda((M_\sigma)_i)$, $i = 1,\ldots,n$ $(E_n[\Lambda((M_\sigma)_i)])$ centered at the correct value.
- S_n^2: The above k-hyper-ellipsoid centered at the the mean of the n estimated values $E_n[\mathbf{v}((M_\sigma)_i)]$.

We have the same cases (excepted S_0) for the analytical method.

5.2 Synthetic data

The above two images have been obtained as projection of 3D-points of a synthetic 3D-scene. In what follows we use this pair of images to study the two proposed methods: the statistical method and the analytical method. In each case we present in a table (Tables 1 and 2) the ratio of the number of realizations lying inside the k-hyper-ellipsoid to the total number of realizations (taking about 1500 realizations). We have done our experimentation for four levels of noise ($\sigma = .5, 1, 2, 3$).

In order to give a direct perception of the results, we provide graphical representation of the uncertainty in the case of epipoles and the epipolar transformation. Unfortunately, due to the high dimensionality it is difficult to visualize the results in the case of the 7-hyper-ellipsoid of uncertainty corresponding to the seven parameters. In each graphical representation we have plotted the estimated ellipse or ellipsoid and, for comparison, also the ellipse or ellipsoid corresponding to the covariance matrix $\Lambda(M)$ obtained by the statistical method from the exact data, which is assumed to be the correct ellipse or ellipsoid.

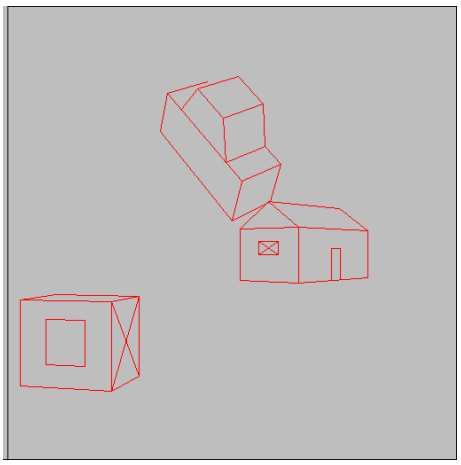

Figure 2: View1 of the synthetic scene

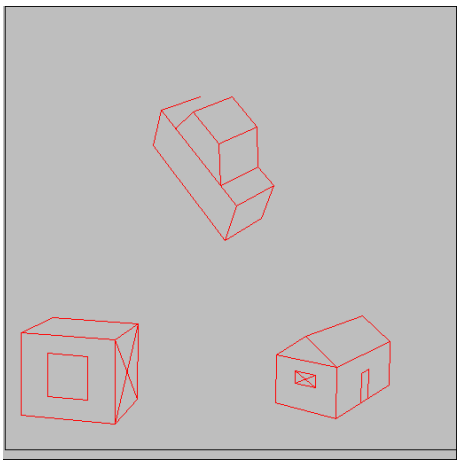

Figure 3: View2 of the synthetic scene

Now let us detail the results presented in Tables 1 and 2. Let us first see the cases where we take the mean of several results (S_n^1,S_n^2,A_n^2 and A_n^2). In the case of the statistical method, we have a good estimation for the epipoles if $\sigma \leq 2$ ($\mathbf{e}$ and $\mathbf{e}'$ in Table 1, Figures 4,6,8 and 10). If we take $\sigma = 3$ we overestimate the uncertainty of the epipoles (Table 1). The uncertainty of the epipolar transformation and the fundamental matrix ($\mathbf{h}$ and $\mathbf{f}$) are more and more overestimated when we increase the level of noise (Table 1, Figures 16 to 19). In the case of the analytical method, the estimation of the epipoles is good enough even in the case of $\sigma = 3$ ($\mathbf{e}$ and $\mathbf{e}'$ in Table 2, Figures 20,22,24 and 26) and the estimation of the epipolar transformation and the fundamental matrix is better than in the case of the statistical method (Table 2, Figures 32 to 35). This is not unreasonable because we have not to forget that we add noise to noisy data and if we add noise of level $\sigma \geq 1$ to data with noise of level $\sigma \geq 1$ the resulting points become very far from the real ones and of course the computed fundamental matrix too. So we conclude from here that it is not a good idea to use the statistical method if the noise level is high.

The tables 1 and 2 also show the results for two randomly chosen examples ($S_{i_1}^1$, $S_{i_1}^2$, $S_{i_2}^1$, $S_{i_2}^2$, $A_{i_1}^1$, $A_{i_1}^2$, $A_{i_2}^1$ and $A_{i_2}^2$) since, in practice, one cannot or does not want to take a mean. In this case, analyzing the plotted k-hyper-ellipsoid is more significant. Unfortunately in the case of the epipolar transformation to plot more than two ellipsoids is useless[2] and for $k > 3$ we have difficulty to plot even one.

In the case of the epipoles, we see that the obtained ellipses are very close one to each other if $\sigma \leq 2$ (Figures 5,7, 9,11,12 to 14,21,23, 25,27 and 28 to 30). If $\sigma = 3$, we see that, in the case of the analytical method, the orientation of the ellipses are preserved but not their size (Figure 31), while, in the case of the statistical method, several ellipses have a

[2] Even two are difficult to distinguish as we see in Figures 32.

completely different form from the expected one. From here we can deduce that if the noise level is ≤ 2 one can use both methods, otherwise it is better to use the analytical one because the statistical method is no more reliable.

5.2.1 Statistical Method

case	($\mathbf{v}$, $\Lambda_{\mathbf{v}}$:)	$\mathbf{v}$	$\sigma = .5$	$\sigma = 1$	$\sigma = 2$	$\sigma = 3$
S_0	($\mathbf{v}(M)$, $\Lambda(M)$)	$\mathbf{e}$	.744	.738	.762	.773
		$\mathbf{e}'$	.747	.743	.765	.753
		$\mathbf{h}$	.751	.778	.816	.902
		$\mathbf{f}$	.762	.766	.798	.865
$S^1_{i_1}$	($\mathbf{v}(M)$, $\Lambda((M_\sigma)_{i_1})$)	$\mathbf{e}$	.737	.777	.774	.967
		$\mathbf{e}'$	.742	.785	.772	.961
		$\mathbf{h}$	.708	.775	.960	.765
		$\mathbf{f}$	.716	.789	.829	.745
$S^1_{i_2}$	($\mathbf{v}(M)$, $\Lambda((M_\sigma)_{i_2})$)	$\mathbf{e}$	.995	.771	.837	.908
		$\mathbf{e}'$	.993	.782	.816	.947
		$\mathbf{h}$	.996	.936	.731	.981
		$\mathbf{f}$	.999	.747	.749	.936
S^1_n	($\mathbf{v}(M)$, $E_n[\Lambda((M_\sigma)_i)]$)	$\mathbf{e}$	.756	.749	.776	.950
		$\mathbf{e}'$	.758	.755	.775	.942
		$\mathbf{h}$	.772	.819	.950	.988
		$\mathbf{f}$	.814	.836	.911	.974
S^2_n	($E_n[\mathbf{v}((M_\sigma)_i)]$, $E_n[\Lambda((M_\sigma)_i)]$)	$\mathbf{e}$	.754	.748	.773	.946
		$\mathbf{e}'$	.750	.746	.774	.948
		$\mathbf{h}$	.776	.821	.953	.988
		$\mathbf{f}$	.811	.840	.912	.978

Table 1: *We compute $n = 50$ matrixes of covariance ($\Lambda((M_\sigma)_{i_1})$ and $\Lambda((M_\sigma)_{i_2})$ are two of them chosen randomly) and their mean ($E_n[\mathbf{v}((M_\sigma)_i)]$). We plot the corresponding k-hyper-ellipsoids and we show $N = 1500$ different realizations. We compute the ratio of the number of realizations lying inside the k-hyper-ellipsoids to the total number of realizations (shown above). Ideally, the ratio should be 0.75.*

Ellipses for e with noise level $\sigma = 1$

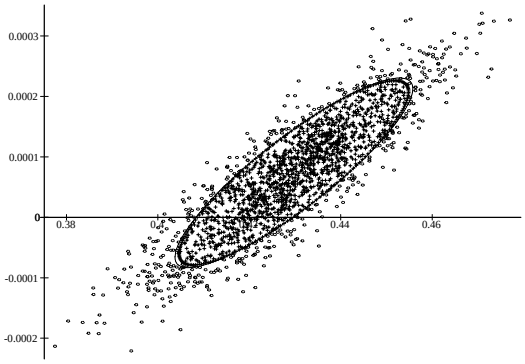

Figure 4: S_0 and S_n^1

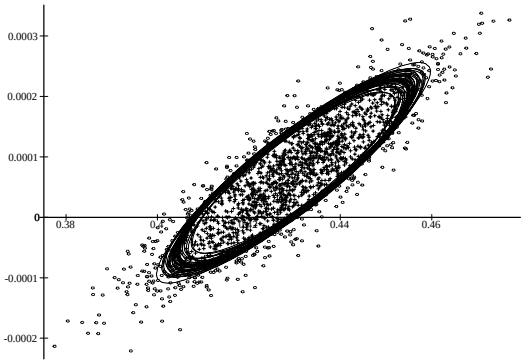

Figure 5: S_0 and S_i^1 $i = 1 \ldots 50$

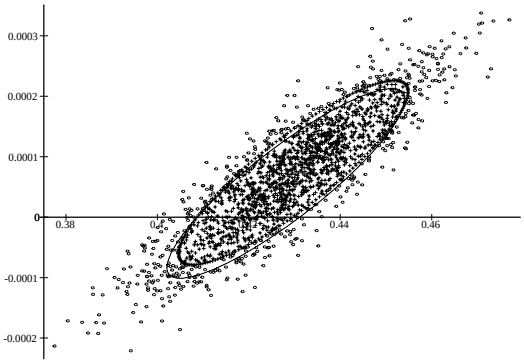

Figure 6: S_0 and S_n^2

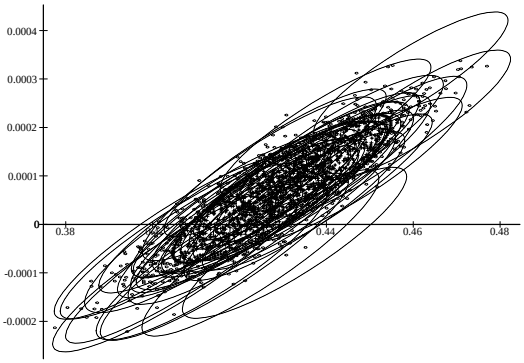

Figure 7: S_0 and S_i^2, $i = 1 \ldots 50$

Ellipses for e′ with noise level $\sigma = .5$

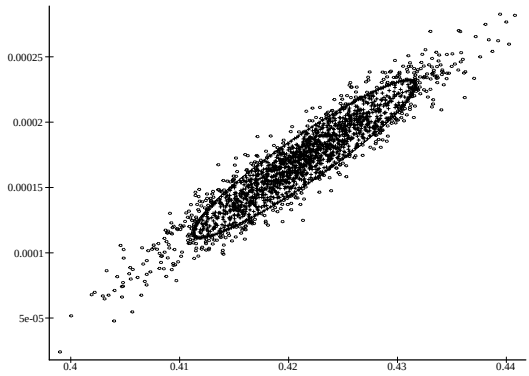

Figure 8: S_0 and S_n^1

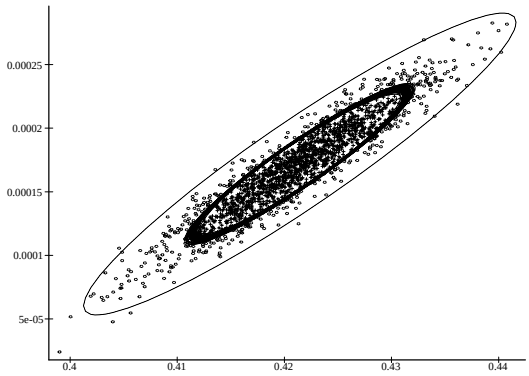

Figure 9: S_0 and S_i^1 $i = 1 \ldots 50$

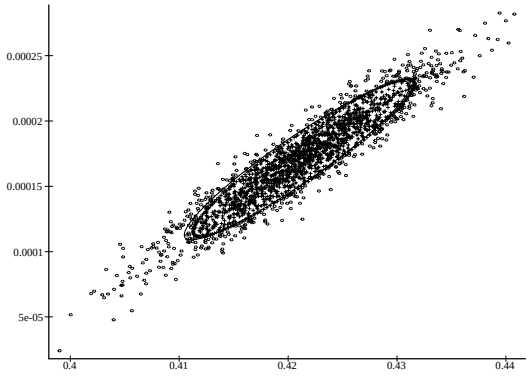

Figure 10: S_0 and S_n^2

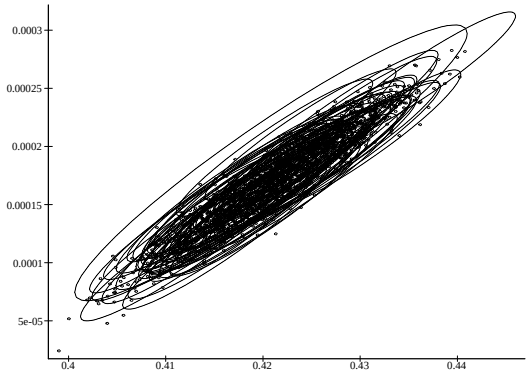

Figure 11: S_0 and S_i^2, $i = 1 \ldots 50$

Ellipses S_0 and S_i^2, $i = 1 \ldots 50$ for e

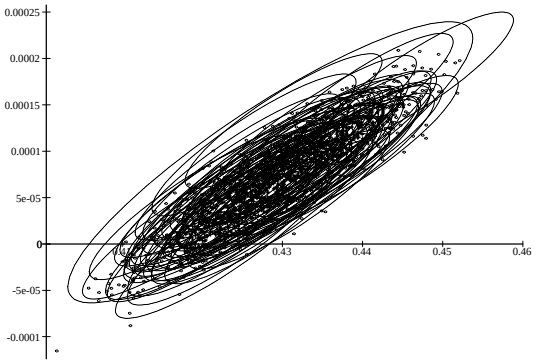

Figure 12: $\sigma = .5$

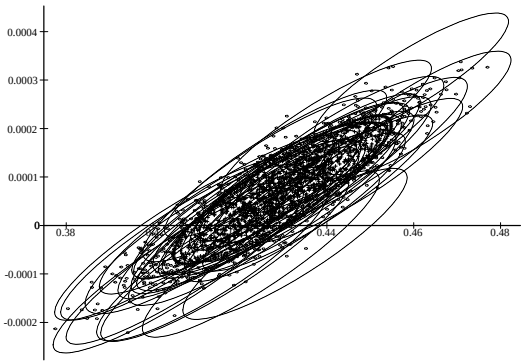

Figure 13: $\sigma = 1$

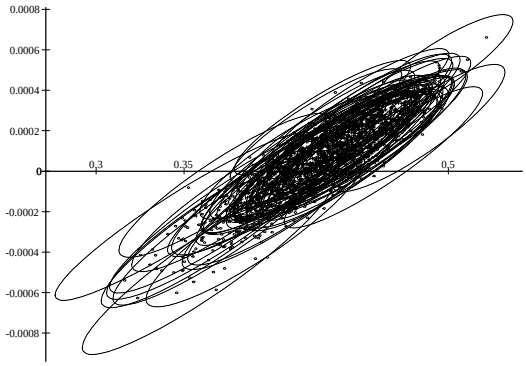

Figure 14: $\sigma = 2$

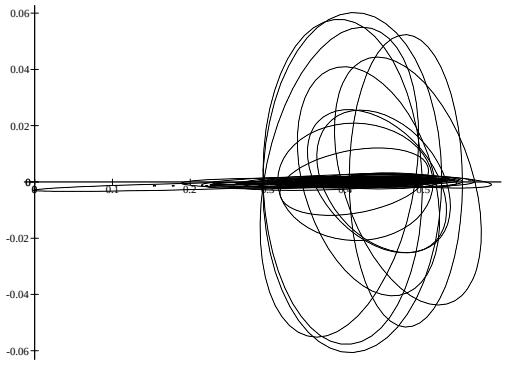

Figure 15: $\sigma = 3$

Ellipsoides S_0 and S_n^2, for h

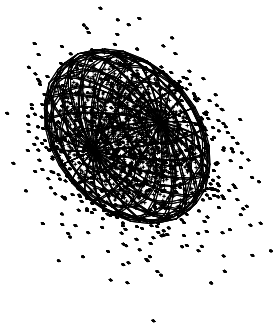

Figure 16: $\sigma = .5$

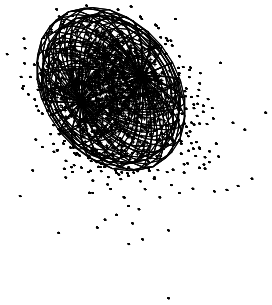

Figure 17: $\sigma = 1$

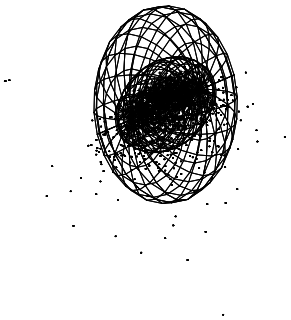

Figure 18: $\sigma = 2$

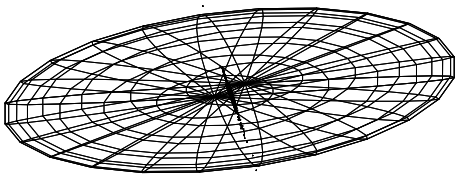

Figure 19: $\sigma = 3$

5.2.2 Analytical Method

case	$(\mathbf{v}, \Lambda_{\mathbf{v}})$	$\mathbf{v}$	$\sigma = .5$	$\sigma = 1$	$\sigma = 2$	$\sigma = 3$
S_0	$(\mathbf{v}(M), \Lambda(M))$	$\mathbf{e}$	.744	.738	.762	.773
		$\mathbf{e}'$	.747	.743	.765	.753
		$\mathbf{h}$	.751	.778	.816	.902
		$\mathbf{f}$	.762	.766	.798	.865
$A^1_{i_1}$	$(\mathbf{v}(M), \Lambda((M_\sigma)_{i_1}))$	$\mathbf{e}$	.778	.804	.719	.651
		$\mathbf{e}'$	.784	.800	.727	.730
		$\mathbf{h}$	.769	.738	.862	.820
		$\mathbf{f}$	.760	.689	.508	.465
$A^1_{i_2}$	$(\mathbf{v}(M), \Lambda((M_\sigma)_{i_2}))$	$\mathbf{e}$	.732	.756	.852	.867
		$\mathbf{e}'$	.734	.758	.852	.878
		$\mathbf{h}$	.826	.809	.837	.815
		$\mathbf{f}$	.682	.642	.651	.545
A^1_n	$(\mathbf{v}(M), E_n[\Lambda((M_\sigma)_i)])$	$\mathbf{e}$	.732	.740	.749	.723
		$\mathbf{e}'$	.732	.745	.745	.719
		$\mathbf{h}$	.747	.765	.826	.983
		$\mathbf{f}$	.760	.801	.820	.904
A^2_n	$(E_n[\mathbf{v}((M_\sigma)_i)], E_n[\Lambda((M_\sigma)_i)])$	$\mathbf{e}$	.736	.732	.741	.715
		$\mathbf{e}'$	.730	.736	.734	.711
		$\mathbf{h}$	.735	.758	.833	.983
		$\mathbf{f}$	.764	.802	.830	.908

Table 2: *We compute $n = 50$ matrixes of covariance ($\Lambda((M_\sigma)_{i_1})$ and $\Lambda((M_\sigma)_{i_2})$ are two of them chosen randomly) and their mean ($E_n[\mathbf{v}((M_\sigma)_i)]$). We plot the corresponding k-hyper-ellipsoids and we show $N = 1500$ different realizations. We compute the ratio of the number of realizations lying inside the k-hyper-ellipsoids to the total number of realizations (shown above). Ideally, the ratio should be 0.75.*

Ellipses for e with noise level $\sigma = 1$

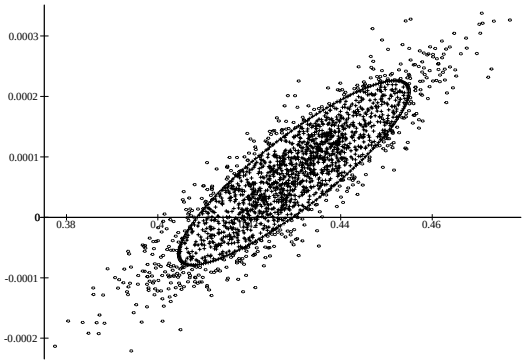

Figure 20: S_0 and A_n^1

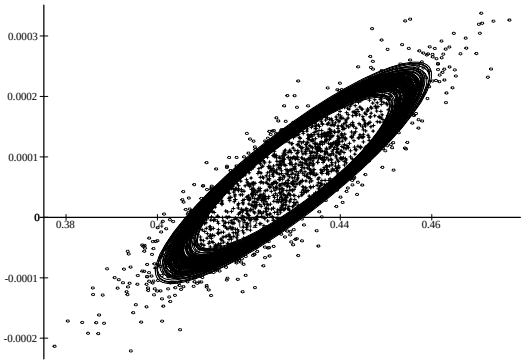

Figure 21: S_0 and A_i^1 $i = 1 \ldots 50$

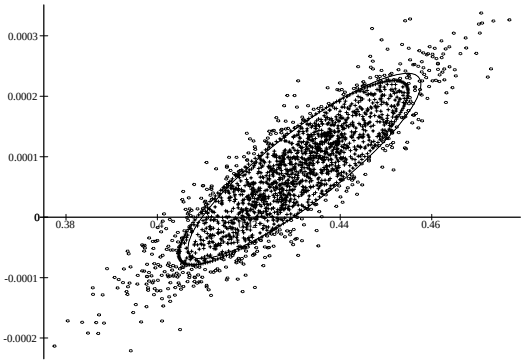

Figure 22: S_0 and A_n^2

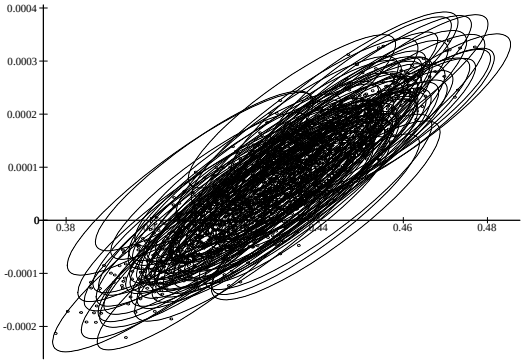

Figure 23: S_0 and A_i^2, $i = 1 \ldots 50$

Ellipses for e′ with noise level $\sigma = .5$

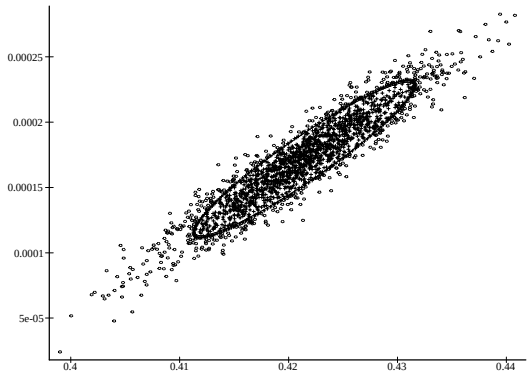

Figure 24: S_0 and A_n^1

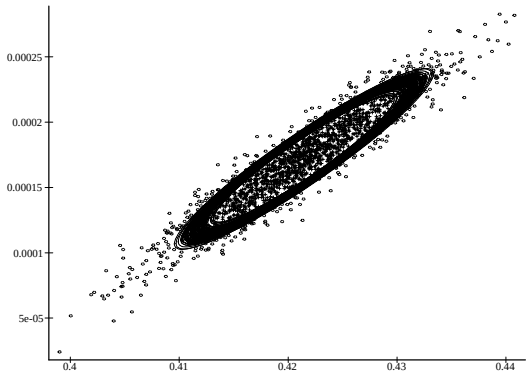

Figure 25: S_0 and A_i^1 $i = 1 \ldots 50$

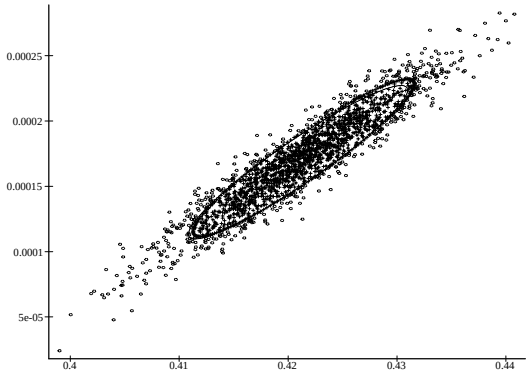

Figure 26: S_0 and A_n^2

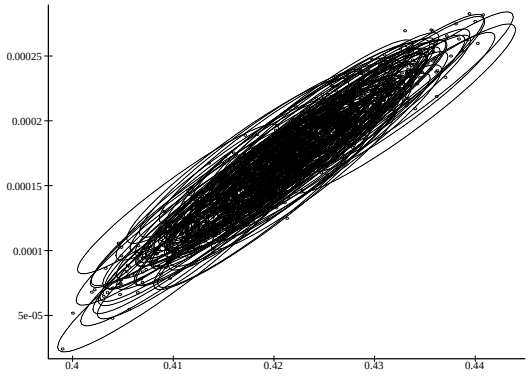

Figure 27: S_0 and A_i^2, $i = 1 \ldots 50$

Ellipses S_0 and A_i^2, $i = 1 \ldots 50$ for e

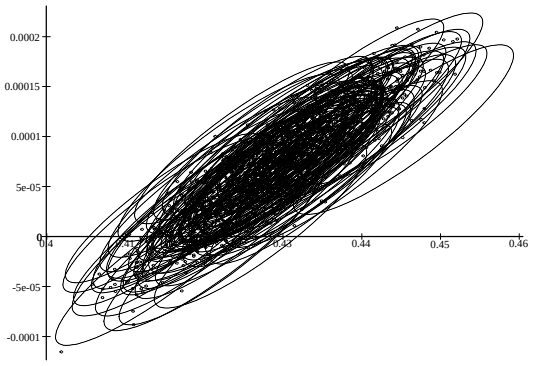

Figure 28: $\sigma = .5$

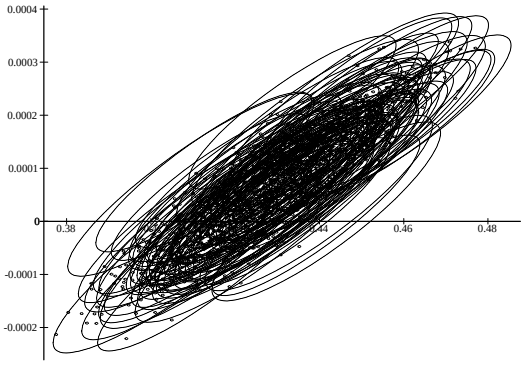

Figure 29: $\sigma = 1.$

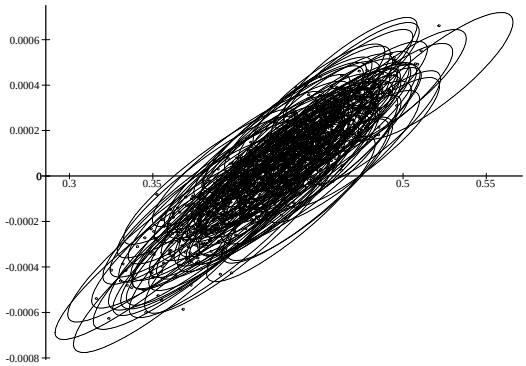

Figure 30: $\sigma = 2.$

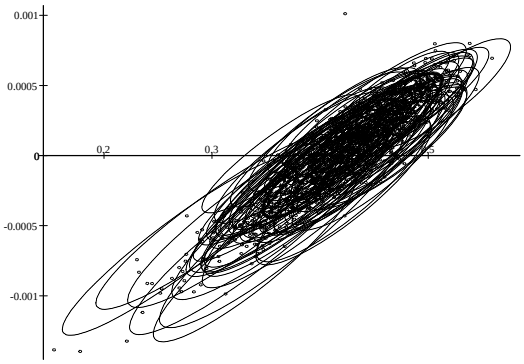

Figure 31: $\sigma = 3.$

Ellipsoids S_0 and A_n^2, for h

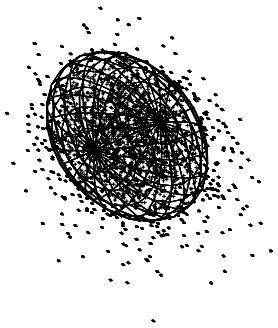

Figure 32: $\sigma = .5$.

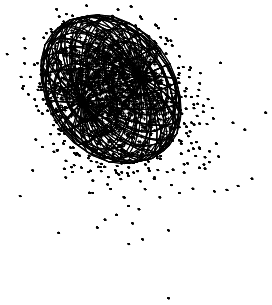

Figure 33: $\sigma = 1$.

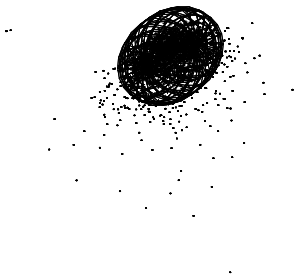

Figure 34: $\sigma = 2$.

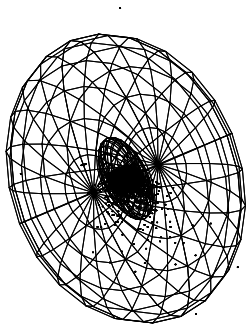

Figure 35: $\sigma = 3$.

5.2.3 Real data

We experimented with several pairs of real images. They are shown in Figures 36,37 and 38 with the point correspondences that have been used.

For each of them, we have first computed, from the point correspondences, the parameters $\mathbf{f}$ of the fundamental matrix and their covariance matrix $\Lambda_{\mathbf{f}}$. The fundamental matrix and its covariance matrix are then easily computable using the following equation

$$\Lambda_{\mathbf{F}} = Dg(\mathbf{f})\Lambda_{\mathbf{f}}Dg(\mathbf{f})^T \tag{20}$$

where $\mathbf{F} = g(\mathbf{f})$ is the funtion which gives $\mathbf{F}$ from the parameters $\mathbf{f}$. Of course the form of g depends of the chosen parametrisation, so we compute the equation (20) as a function of this parameterization. Several epipolar lines are shown in the figures to give an idea of the position of the epipoles.

The tables 3, 4 and 5 show the obtained fundamental matrices $\mathbf{F}$ and $\mathbf{F}'$. $\mathbf{F}$ represents the fundamental matrix obtained by using the nonlinear method without outliers rejection and $\mathbf{F}'$ the fundamental matrix obtained by the outliers rejection method. For both methods we computed the covariance matrices using first the analytical method ($\Lambda^a_{\mathbf{F}}$ and $\Lambda^a_{\mathbf{F}'}$) and then the statistical method ($\Lambda^s_{\mathbf{F}}$ and $\Lambda^s_{\mathbf{F}'}$). Of course these are 9×9 matrices but we decided to show only their diagonal elements which are enough to estimate the size of the uncertainty by comparing them to the elements of the fundamental matrix. We have to mention here that obviously the fundamental matrix is normalized, we could not speak otherwise about an uncertainty.

In the case of the statistical method we estimated that we have noise of level .2, in the case of the figure 36 where we know the points position with a subpixel precision and 1, in the other cases. Each time we added noise to our points correspondences and computed the covariance $\Lambda((M_\sigma)_{i_1})$. As we saw in the case of the synthetic data if we want to improve this we repeat this process several times and take the mean $E[\Lambda((M_\sigma)_{i_1})]$.

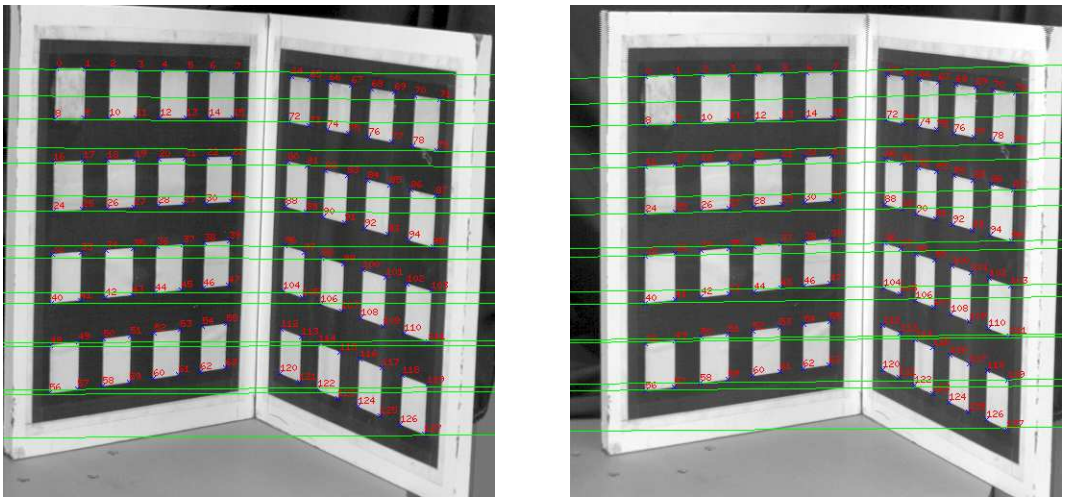

Figure 36: First pair of real images.

(i,j)	$\mathbf{F}$	$\Lambda^a_{\mathbf{F}}$	$\Lambda^s_{\mathbf{F}}$	$\mathbf{F}'$	$\Lambda^a_{\mathbf{F}'}$	$\Lambda^s_{\mathbf{F}'}$
(1,1)	-9.319e-08	1.829e-16	2.905e-12	-8.973e-08	1.835e-16	1.043e-15
(1,2)	6.792e-06	3.172e-13	1.169e-11	6.605e-06	3.185e-13	1.811e-12
(1,3)	-2.167e-03	2.013e-08	2.123e-04	-2.118e-03	2.023e-08	1.132e-07
(2,1)	2.605e-07	3.299e-13	1.091e-11	4.537e-07	3.313e-13	1.891e-12
(2,2)	1.275e-07	1.460e-15	4.214e-14	1.268e-07	1.463e-15	9.029e-15
(2,3)	-7.592e-02	2.097e-07	1.607e-05	-7.609e-02	2.110e-07	1.167e-06
(3,1)	-1.084e-03	2.403e-08	3.262e-04	-1.139e-03	2.414e-08	1.355e-07
(3,2)	7.291e-02	2.149e-07	1.494e-05	7.308e-02	2.161e-07	1.203e-06
(3,3)	9.944e-01	4.736e-09	3.473e-07	9.944e-01	4.788e-09	2.656e-08

Table 3: The fundamental matrices and their covariance matrices for the first pair of images.

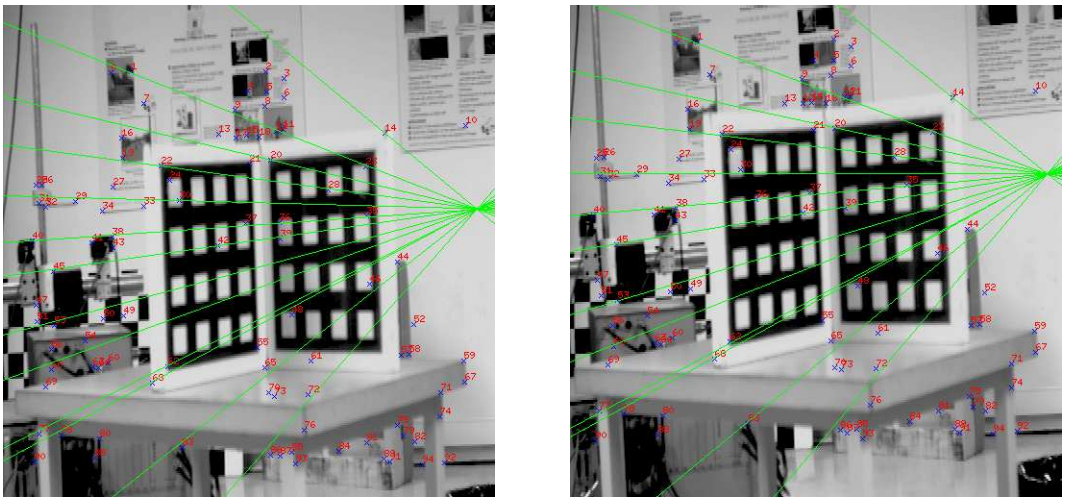

Figure 37: Second pair of real images.

(i,j)	$\mathbf{F}$	$\Lambda^a_{\mathbf{F}}$	$\Lambda^s_{\mathbf{F}}$	$\mathbf{F}'$	$\Lambda^a_{\mathbf{F}'}$	$\Lambda^s_{\mathbf{F}'}$
(1,1)	-1.325e-06	1.092e-14	2.713e-14	-1.324e-06	1.093e-14	9.751e-14
(1,2)	1.430e-04	2.240e-11	1.246e-10	1.430e-04	2.242e-11	9.461e-10
(1,3)	-1.454e-02	3.302e-07	1.878e-06	-1.453e-02	3.304e-07	1.585e-05
(2,1)	-1.432e-04	2.309e-11	1.260e-10	-1.432e-04	2.311e-11	9.183e-10
(2,2)	-2.134e-06	1.526e-13	3.725e-13	-2.135e-06	1.528e-13	8.0135e-13
(2,3)	7.077e-02	1.212e-06	2.708e-06	7.077e-02	1.213e-06	4.16e-06
(3,1)	1.325e-02	2.892e-07	1.531e-06	1.325e-02	2.894e-07	1.288e-05
(3,2)	-7.081e-02	1.005e-06	2.241e-06	-7.081e-02	1.006e-06	3.533e-06
(3,3)	9.948e-01	2.478e-08	5.760e-08	9.948e-01	2.479e-08	1.216e-07

Table 4: The fundamental matrices and their covariance matrices for the second pair of images.

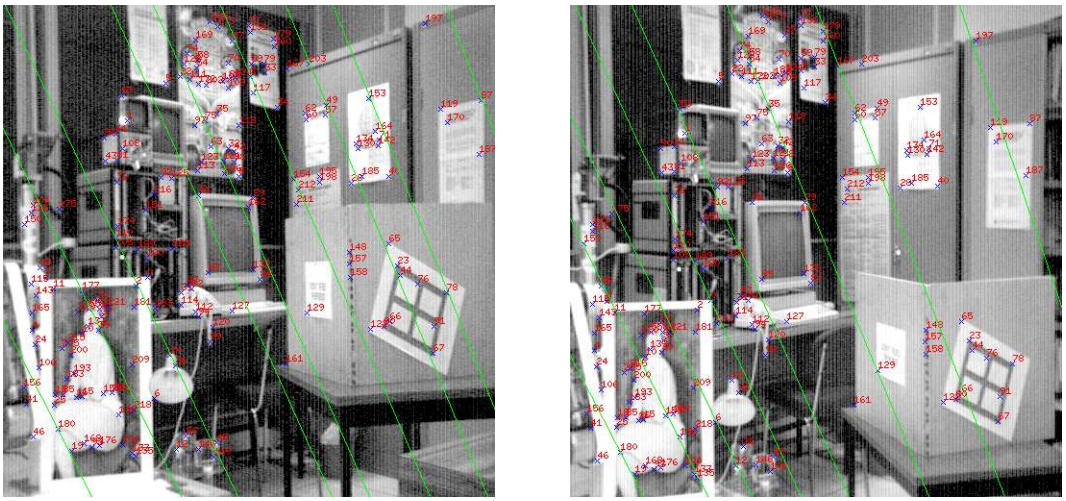

Figure 38: Third pair of real images.

(i,j)	$\mathbf{F}$	$\Lambda^a_{\mathbf{F}}$	$\Lambda^s_{\mathbf{F}}$	$\mathbf{F}'$	$\Lambda^a_{\mathbf{F}'}$	$\Lambda^s_{\mathbf{F}'}$
(1,1)	6.722e-06	8.854e-14	3.318e-13	6.722e-06	8.854e-14	3.278e-13
(1,2)	-1.743e-05	1.578e-11	6.265e-11	-1.743e-05	1.578e-11	6.534e-11
(1,3)	6.842e-02	2.308e-06	8.631e-06	6.842e-02	2.309e-06	8.041e-06
(2,1)	1.837e-06	1.291e-11	5.166e-11	1.837e-05	1.291e-11	5.356e-11
(2,2)	-2.044e-06	3.082e-14	1.098e-13	-2.044e-06	3.082e-14	1.104e-13
(2,3)	-3.193e-02	1.296e-06	5.039e-06	-3.193e-02	1.296e-06	8.502e-07
(3,1)	-7.023e-02	2.075e-06	7.729e-06	-7.023e-02	2.075e-06	7.241e-06
(3,2)	3.303e-02	1.437e-06	5.574e-06	3.303e-02	1.437e-06	5.706e-06
(3,3)	9.941e-01	6.770e-08	2.524e-07	9.941e-01	6.770e-08	2.394e-07

Table 5: The fundamental matrices and their covariance matrices for the third pair of images.

6 Conclusion

A fundamental matrix determines completely the epipolar geometry between two images, which allows 3D projective reconstruction or 3D invariants computation. However, the precision of the estimated fundamental matrix depends upon a number of factors, for example, the number of point correspondences, the configuration of points or the precision of the extracted points. Thus a key issue is to characterize correctly the uncertainty of the fundamental matrix in order to use it appropriately in the subsequent stages.

In this paper, we have presented two methods for estimating the covariance matrix of the fundamental matrix. The first method assumes that the noise level of data points is known, which implies that the precision of the corner detector used has to be estimated. Then, by simulation, we carry out a sufficiently large number of experiments by adding independent noise to data points. A fundamental matrix is estimated for each experiment, and finally the covariance matrix is estimated through classical statistical techniques. The second method is more general, which only assumes that the noise in each data point is independent and identically distributed. The covariance matrix is estimated through a first order approximation. If the noise level of data points is known, the first method can be used, which usually yields better results than the second one. However the first method is computationally very expensive and the noise level is usually not known in practice; it is thus merely of theoretical importance. In this paper, we have used synthetic data with known level noise, and compared two methods. It appears that, if the noise level is moderate (the standard deviation is less than two pixels), the two methods yield very similar results, which implies that the first order approximation used in the second method is reasonable. The two methods have also been validated with real data.

Future work will consist in using the covariance matrix of the fundamental matrix estimated with the second method for projective reconstruction and computation of three-dimensional invariants.

References

[Fau93] Olivier Faugeras. *Three-Dimensional Computer Vision: a Geometric Viewpoint.* The MIT Press, 1993.

[FLM92] Olivier Faugeras, Tuan Luong, and Steven Maybank. Camera self-calibration: theory and experiments. In G. Sandini, editor, *Proceedings of the 2nd European Conference on Computer Vision*, volume 588 of *Lecture Notes in Computer Science*, pages 321–334, Santa Margherita Ligure, Italy, May 1992. Springer-Verlag.

[Har95] R.I. Hartley. In defence of the 8-point algorithm. In *Proceedings of the 5th Proc. International Conference on Computer Vision*, Boston, MA, June 1995. IEEE Computer Society Press. To appear.

[HGC92] Richard Hartley, Rajiv Gupta, and Tom Chang. Stereo from uncalibrated cameras. In *Proceedings of the International Conference on Computer Vision and Pattern Recognition*, pages 761–764, Urbana Champaign, IL, June 1992. IEEE.

[LF94] Quang-Tuan Luong and Olivier Faugeras. A stability analysis of the fundamental matrix. In J-O. Eklundh, editor, *Proceedings of the 3rd European Conference on Computer Vision*, volume 800-801 of *Lecture Notes in Computer Science*, pages 577–588, Stockholm, Sweden, May 1994. Springer-Verlag.

[LH81] H.C. Longuet-Higgins. A Computer Algorithm for Reconstructing a Scene from Two Projections. *Nature*, 293:133–135, 1981.

[Luo92] Quang-Tuan Luong. *Matrice Fondamentale et Calibration Visuelle sur l'Environnement-Vers une plus grande autonomie des systèmes robotiques.* PhD thesis, Université de Paris-Sud, Centre d'Orsay, December 1992.

[Ols92] S.I. Olsen. Epipolar line estimation. In *Proceedings of the 2nd European Conference on Computer Vision*, pages 307–311, Santa Margherita Ligure, Italy, May 1992.

[PFTV88] William H. Press, Brian P. Flannery, Saul A. Teukolsky, and William T. Vetterling. *Numerical Recipes in C.* Cambridge University Press, 1988.

[ZDFL94] Zhengyou Zhang, Rachid Deriche, Olivier Faugeras, and Quang-Tuan Luong. A robust technique for matching two uncalibrated images through the recovery of the unknown epipolar geometry. *Artificial Intelligence Journal*, 1994. to appear. Also INRIA Research Report No.2273, May 1994.

[ZF92] Zhengyou Zhang and Olivier D. Faugeras. *3D Dynamic Scene Analysis: A Stereo Based Approach.* Springer, Berlin, Heidelberg, 1992.

Unité de recherche INRIA Lorraine, Technopôle de Nancy-Brabois, Campus scientifique,
615 rue du Jardin Botanique, BP 101, 54600 VILLERS LÈS NANCY
Unité de recherche INRIA Rennes, Irisa, Campus universitaire de Beaulieu, 35042 RENNES Cedex
Unité de recherche INRIA Rhône-Alpes, 46 avenue Félix Viallet, 38031 GRENOBLE Cedex 1
Unité de recherche INRIA Rocquencourt, Domaine de Voluceau, Rocquencourt, BP 105, 78153 LE CHESNAY Cedex
Unité de recherche INRIA Sophia-Antipolis, 2004 route des Lucioles, BP 93, 06902 SOPHIA-ANTIPOLIS Cedex

Éditeur
INRIA, Domaine de Voluceau, Rocquencourt, BP 105, 78153 LE CHESNAY Cedex (France)
ISSN 0249-6399